Role of anatomic liver compartments in relaxivity-iron relationships

N. R. Ghugre[1,2], I. Gonzalez[3], E. Butensky[4], R. Fischer[5,6], R. Williams[7], P. Harmatz[4], T. D. Coates[8], and J. C. Wood[1,2]

[1]Division of Cardiology, Childrens Hospital Los Angeles, Los Angeles, CA, United States, [2]Department of Radiology, Childrens Hospital Los Angeles, Los Angeles, CA, United States, [3]Department of Pathology, Childrens Hospital Los Angeles, Los Angeles, CA, United States, [4]Department of Gastroenterology and Nutrition, Childrens Hospital and Research Center at Oakland, Oakland, CA, United States, [5]Pediatric Clinical Research Center, Childrens Hospital and Research Center at Oakland, Oakland, CA, United States, [6]Department of Pediatric Hematology-Oncology, University Clinic Hamburg-Eppendorf, Hamburg, Germany, [7]Department of Pathology, Childrens Hospital and Research Center at Oakland, Oakland, CA, United States, [8]Division of Hematology-Oncology, Childrens Hospital Los Angeles, Los Angeles, CA, United States

Introduction: In order to monitor tissue iron stores, MRI is slowly replacing the need to biopsy patients with sickle cell disease and β-thalassemia. R2 (1/T2) and R2* (1/T2*) calibrations for hepatic iron concentration (HIC) have been obtained within bounds of clinical accuracy (1, 2). These calibrations have been based on unchelated or deferoxamine chelated patients. Deferoxamine removes iron equally from hepatocyte and sinusoidal compartments of the liver. On the other hand, limited animal studies have suggested that novel oral chelators like deferasirox mobilize iron differently in the two compartments and hence alter the R2-iron calibration curve. From a clinical standpoint it is very important to understand the trend of R2 as a function of the type of chelation therapy that a patient is undergoing. Toward this end, our study focuses on 1) characterizing relative iron loading in the hepatocyte and sinusoidal liver compartments as a function of HIC and 2) systematically testing the contributions of the two iron pools in the relaxivity-iron relationships by computational modeling. We hypothesize that by introducing the larger sinusoidal iron structures (~10μm), 1) R2 will drop at lower HIC due to static refocusing and 2) at higher HIC, differences will be less dramatic due to relative abundance of smaller iron clusters.

Methods: Iron storage pattern was interrogated in 43 liver biopsies from patients with sickle cell disease and β-thalassemia. The histologic sections were evaluated by an experienced pathologist to assess relative iron distribution in heaptocytes and Kupffer cells (sinusoids), based on scoring developed by Deugnier et. al. (3). Iron scores for each compartment were then represented as a percentage of total iron score. Each biopsy sample was also sent to Mayo Clinic for quantitative iron assessment.

Realistic liver geometries were simulated in the form of a 80 μm block consisting of 64 cuboidal hepatocytes (4). The sinusoidal regions were represented as 18 cylindrical regions with diameter=10 μm and height=20 μm. They were located at the intersection of adjacent hepatocytes, similar to that observed in liver parenchyma. The total volume of the cylinders was ~6% compared to the virtual liver environment, which is roughly equal to that stated in the literature. Iron spheres were distributed for two types of geometries 1) without sinusoids and 2) with sinusoids based on the relative iron scoring. R2 and R2* imaging experiments were then simulated as described previously (4). 5000 water protons performed a random walk thorugh this environment and their phase accruals were converted into field induction decays. R2 and R2* values were computed for HIC ranging from 0.5-40 mg/g dry tissue weight.

Results: Fig. 1 shows sinusoid (SIS) and hepatocyte iron scores (HIS) as a percentage of total iron scores for all the evaluated liver biopsies. The fit on HIS was chosen to decide the relative fill fraction of iron in the sinusoidal and hepatocyte compartments of the model. The percentage of iron in the hepatocytes was given by, %HIS = exp(3.5669345 + 0.1857491*log(HIC)). Fig. 2 (a) shows a light micrograph (9000X) from representative patient with HIC = 57.8 mg/g and (b) shows a 4 μm thick section of a simulated liver geometry. Blue stain represents the iron deposits and the arrows indicate sinusoidal iron compartments; note the striking resemblance in 'blueness' distribution in (a) and (b). Fig. 3 shows a side-by-side comparison of predicted R2 with and without sinusoids; sinusoidal iron dropped R2 closer to the St. Pierre calibration curve (1). While differences between the two liver geometries were less apparent at higher iron burdens (~7.6%), they were more pronounced for HIC<15 mg/g (~15.5%). This may be further appreciated from Fig. 4 which provides an alternate view for the same observation. Here the predicted HIC (based on R2 value) is plotted against 'true' HIC (St. Pierre calibration); note how close the sinusoids bring R2 to the line of unity.

Discussion: Although Harmatz et. al (5) have previously reported mean iron scoring patterns in different compartments of the liver, a storage classification based on patient iron burden had not been performed. The relative iron loading clearly demonstrated that in transfusional iron overload syndromes, iron is first deposited in the sinusoids (HIC<5 mg/g) and then is propagated into the hepatocytes (HIC > 5 mg/g). R2 is highly sensitive to magnetic organization of tissue iron. A realistic anatomic model can hence detect relaxivity changes brought about by different iron compartments. Such a multi-compartment model can be very useful to recreate scenarios for other types of iron over load syndromes. For example, in Hemochromatosis Type 1, 2 and 3, iron is loaded only in the hepatocytes while in Type 4, only the sinusoids are loaded. Each iron overload model will have a characteristic R2-iron relationship which can act as a signature for the different types of overload. Furthermore, chelator response can also be studied; the anatomic model can be subjected to an oral chelator that removes iron from the hepatocytes but maintains sinusoidal iron. Established R2-iron responses for all these scenarios will be greatly beneficial for efficient patient care and management. A model-based approach will eliminate the need to rescan and recalibrate patients for changes in treatment or imaging conditions.

Acknowledgements: GCRC (RR00043-43), NIH (1 R01 HL75592-01A1), Saban Research Institute (CHLA), The Wright Foundation.

References: 1) St Pierre TG, Clark PR, Chua-anusorn W, et al., Blood 2005; 105:855-861.
2) Wood JC, Enriquez C, Ghugre N, et al., Blood 2005; 106:1460-1465.
3) Deugnier YM, et. al., Gastroenterology. 1992 Jun; 102(6):2050-9.
4) Ghugre N, et. al. Proc. Intl. Soc. Mag. Reson. Med 15, 2007; 1780.
5) Harmatz P, Butensky E, et. al., Blood. 2000 Jul 1;96(1):76-9.

Figure 1

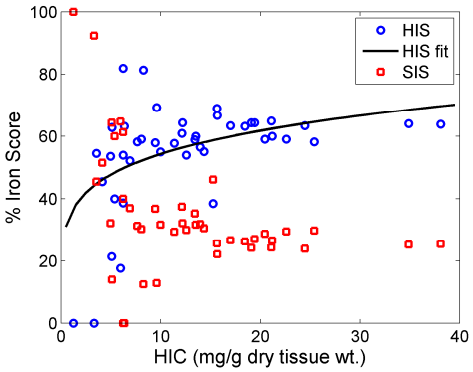

(a) **Figure 2** **(b)**

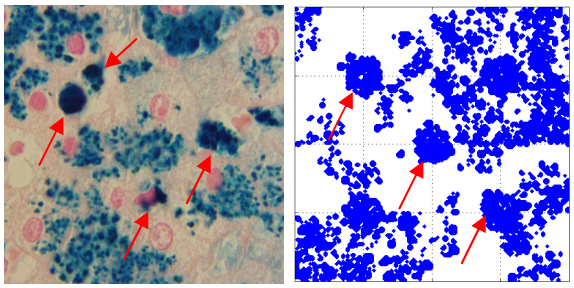

Figure 3

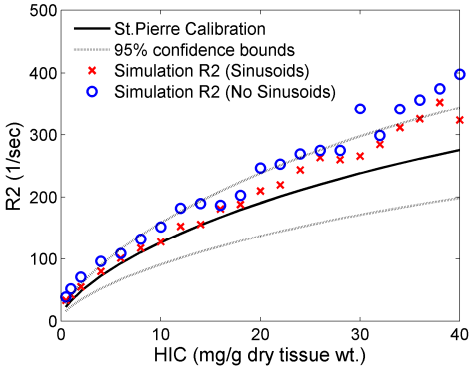

Figure 4